

# A Micromanipulation System for Single Cell Deposition

Zhe Lu, Christopher Moraes, Yan Zhao, LiDan You, Craig A. Simmons, and Yu Sun

**Abstract**—Many microfabricated devices have been developed to quantify cellular response to a multitude of stimuli at a single-cell level in a high throughput manner. These single-cell studies require cells to be individually positioned at defined locations on a microdevice. This paper presents a micromanipulation system for automated pick-place of single cells. Integrating computer vision and motion control algorithms, the system visually tracks a cell in real time and controls multiple motion devices coordinately. Via fine manipulation of picoliter fluids and pressure of a few Pascals, the system accurately picks up a single cell, transfers the cell, and deposits it at a target location at a speed of 15-30 sec/cell. The micromanipulation system has the advantages of non-invasiveness, high specificity, and high precision. It is suitable to pick-place both non-labeled and labeled cells and applicable to standard cell culture substrates and microdevices with an open top.

## I. INTRODUCTION

Population-based studies in biological experimentation are limited by the ensemble averaging of individual cellular response. These population-based studies do not permit a thorough examination of the stochastic processes involved in regulating cellular function at the single cell level, calling for the ability to manipulate single cells for investigating single-cell behavior.

Biological cells are sensitive to factors in the cell culture environment, such as chemical, matrix, and mechanical stimulation. Single cell culture has been shown to substantially affect cellular response to these factors. Recent advances in microdevice technologies have enabled rapid screening of cellular response to a variety of environmental factors, including cell-biomaterial interactions [1], chemical stimulation [2], extra-cellular matrix proteins [3], and dynamic mechanical stimulation [4]. These systems have significant applications in drug discovery, tissue engineering, and fundamental cell biology. For single-cell studies, cells must be individually positioned at defined locations on a microfabricated device.

Current techniques are limited in the ability of positioning individual cells and lack specificity. Chemical modification to produce patterned adhesion sites is a widely used approach [5]. However, non-specific binding often occurs, and efficiently ‘catching’ a single cell requires adherent spots too small to allow for the cell to spread and maintain normal function. The use of microfabricated wells [6], vacuum arrays [7], dielectrophoresis [8], or hydrodynamic trapping structures [9] requires modifications to the design and microfabrication processes of a microdevice, and in certain

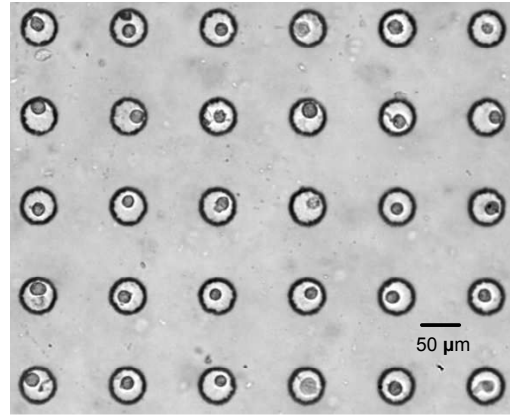


Fig. 1. Cells deposited into a 5×6 microfabricated wells using the robotic micromanipulation system.

cases, can interfere with proper operation of the platform. The physical structures built on the microdevice for single cell manipulation can also impact long-term cell adhesion and function. Other techniques such as optical trapping [10], acoustic wave manipulation [11], and magnetic localization [12] require dedicated, often expensive equipment which can be technically challenging to operate and is not available in most labs.

An automated cell deposition system (CyCLONE, Beckman Coulter Inc.) is commercially available for depositing single cells into standard multi-well plates. As an additional module of an expensive flow cytometer, the CyClone system requires large sample volumes and cells to be labeled/tagged with fluorescence dyes/proteins. Cells for which specific cell-surface antibodies have not been developed, and cells that are sensitive to labeling cannot be manipulated by the instrument. Additionally, since the system was developed for multi-well plates that have a large well size/pitch, the positioning accuracy is limited to  $\sim 100 \mu\text{m}$ .

Microrobotic pick-place of single cells promises advantages of non-invasiveness, high specificity, high precision, and applicability to any microfabricated devices with an open top without requiring modifications to device design and fabrication processes. It is suitable for use when sample volumes are limited and is applicable to manipulate both labeled and non-labeled cells. A robotic system was recently demonstrated for the pick-place of single cells [13]. Although the positioning of a micropipette was automated, the cell aspiration and deposition steps were based on trial and error. Automatically aspirating and dispensing a single cell requires control strategies for precision control of picoliter volume of

The authors are with Dept. of Mechanical and Industrial Engineering, University of Toronto, 5 King's College Road, Toronto, ON, Canada, M5S 3G8. sun@mie.utoronto.ca

liquid at varying flow velocities. The lack of such control strategies limits system operation speed and reproducibility.

In this paper, we present a microrobotic system that is capable of precisely aspirating and depositing single live cells. The micromanipulation system only requires a motorized micromanipulator, micropipette, and a precision linear stage. Computer vision and motion control algorithms are built in the system for pick-place of cells. This paper presents the micromanipulation technique as well as the application of the system to deposit single cells on three types of microfabricated device arrays, with one deposition result shown in Fig. 1.

## II. SYSTEM DESIGN

Automation of aspirating and depositing single cells is made possible by integrating: (i) a computer-controlled linear stage for precisely adjusting cell aspiration and dispensing picoliter fluids or pressure of a few Pa; (ii) computer vision and motion control algorithms for tracking cells and coordinately controlling multiple motion control devices.

### A. System Architecture

As shown in Fig. 2(a), a microfabricated device is placed on an  $X$ - $Y$  motorized stage (*ProScan<sup>TM</sup>*, Prior Scientific Inc.) that is mounted on a standard inverted microscope. The travel range along both axes is 75 mm with a resolution of  $0.01 \mu\text{m}$ . A CMOS camera is used with the microscope to provide visual feedback. A glass micropipette, pulled and forged, is connected to a 3-DOF motorized micromanipulator (MP285, Sutter Inc.) that has a travel range of 25 mm and a  $0.04 \mu\text{m}$  positioning resolution along each axis. The micropipette is connected to a  $25 \mu\text{l}$  glass syringe. A linear stage (eTrack, Newmark Systems Inc.) is used to control the movement of the plunger inside the syringe for adjusting aspiration and dispensing volume. The resolution of the linear stage is  $0.04 \mu\text{m}$ . A host computer coordinately controls the  $X$ - $Y$  stage, linear stage, and micromanipulator. Fig. 2(b) shows a picture of the system.

### B. Overall Operation Sequence

A small volume of a cell sample is deposited in the proximity of deposition destinations (Fig. 3). The first microwell is denoted by  $W(1,1)$ , and the center position of  $W(1,1)$  in the  $X$ - $Y$  stage frame is denoted by  $P_A=(x_0, y_0)$ .  $\Delta x$  and  $\Delta y$  are pitches between two adjacent microwells.  $m$  and  $n$  represent the order of microwells along the  $X$  and  $Y$  directions. The center position of microwell  $W(i, j)$  is then  $(x_0 + (i-1)\Delta x, y_0 + (j-1)\Delta y)$ , where  $1 \leq i \leq m$  and  $1 \leq j \leq n$ .

System operation starts with vision-based contact detection [14] to determine the vertical positions of the micropipette tip and surface of the microfabricated device. Controlled by the micromanipulator, the position of the micropipette tip is set to  $30 \mu\text{m}$  above the microdevice surface and  $20 \mu\text{m}$  left to the center of the field of view of the microscope. When area B is brought into the field of view, a user selects an appropriate cell for transfer via computer mouse clicking. The system then recognizes the cell through

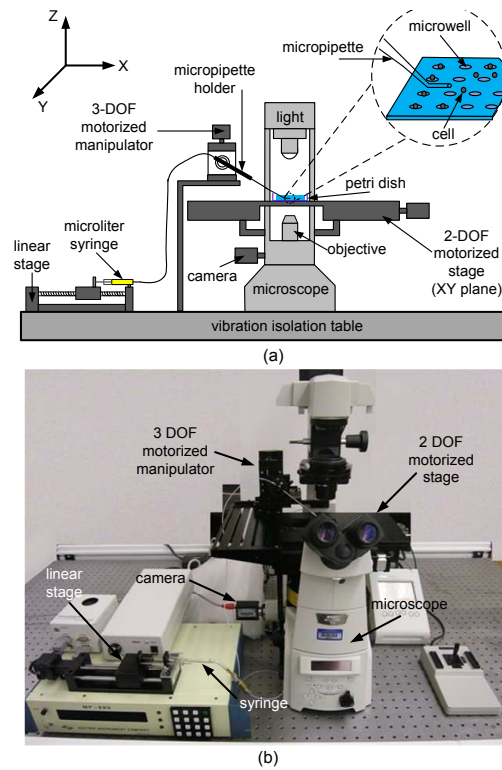


Fig. 2. Micromanipulation system for single cell deposition. (a) Schematic illustration. (b) Picture.

image processing and brings the cell to the center of the field of view. The position of the cell in the  $X$ - $Y$  frame is recorded as  $P_B$  for the system to remember accurately the location of cell sources in area B.

The micropipette is automatically controlled to move downwards to vertically align with the target cell. After aspirating/picking up the cell, the system lifts the micropipette  $30 \mu\text{m}$  above the microdevice surface, and moves the center of microwell  $W(i, j)$  to the center of the field of view. The micromanipulator lowers the micropipette, and the linear stage is triggered to control the application of a fine pressure to deposit the cell into the target microwell. For the next cycle,  $P_B$  is moved to the center of the field of view for the user to select the next appropriate cell for transfer to a microwell. This process is repeated until the entire array of microwells is filled.

## III. AUTOMATED CELL PICK-PLACE

### A. Fluid Dynamics within Micropipette

One type of glass micropipettes used for pick-place of cells is schematically shown in Fig. 4(a). The micropipette has a bending angle of  $30^\circ$  and a horizontal tip of 1mm in length. The tip diameter can be precisely tailored during micropipette processing to accommodate different cell types. The micropipette is filled with mineral oil from the syringe. When the micropipette is half filled with mineral oil, its tip is immersed into cell medium. A small amount of cell medium flows from the micropipette opening into the micropipette

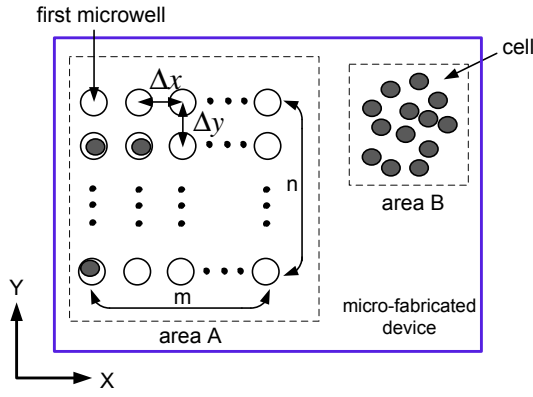


Fig. 3. An example microwell array on a microfabricated device. Single cells are transferred from area B into microwells. Each microwell must contain one and only one cell.

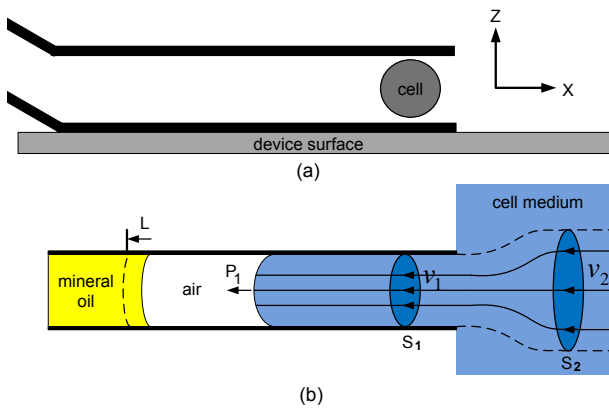


Fig. 4. (a) Micropipette with a horizontal tip to aspirate cells inside the micropipette. (b) Fluid dynamics in the micropipette tip.

tip (Fig. 4(b)). When air-liquid equilibrium is reached inside the micropipette, fluid velocity at the micropipette opening is zero.

Let  $P_0$ ,  $V_0$  be the pressure and volume of the air bubble before aspiration. When aspirated, the oil-air interface moves to the left by a distance,  $L$ . The pressure and volume of the air bubble then become  $P_1$  and  $V_1$ . Since the temperature of the air bubble does not change during aspiration,  $P_0V_0 = P_1V_1$ . Because  $V_1 > V_0$ ,  $P_1 < P_0$ .

As the pressure in the air bubble decreases during aspiration, more cell medium flows into the micropipette. Let  $S_1$  be the cross sectional area of the micropipette tip,  $v_1$  be the fluid velocity at  $S_1$ , and  $d$  be the density of cell medium. The mass flow rate at  $S_1$  is  $S_1v_1d$ . In the proximity outside the micropipette tip, cell medium inside the dashed lines responds to aspiration. The flow change from the outside to the inside of the micropipette tip is continuous and gradual, maintaining laminar flow. Let  $S_2$  be a cross sectional area outside the micropipette tip and  $v_2$  be the fluid velocity at  $S_2$ . According to the law of conservation of mass,  $S_1v_1d = S_2v_2d$ , then  $v_1 = v_2 \frac{S_2}{S_1}$ .

Since  $\frac{S_2}{S_1} \gg 1$ , fluid velocity increases dramatically after cell medium is aspirated into the micropipette tip. Because

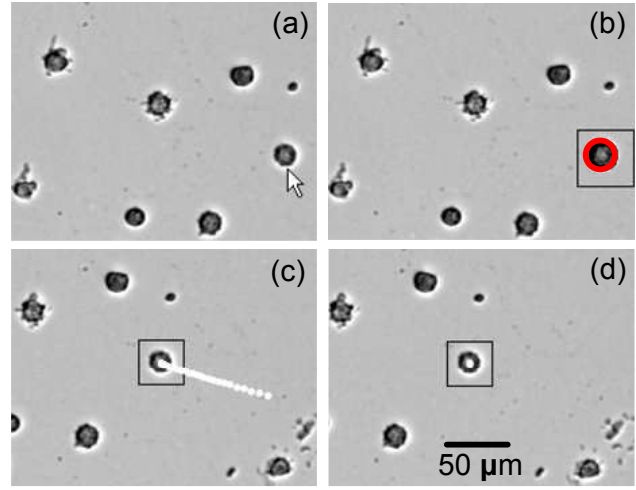


Fig. 5. Image sequence of cell recognition and tracking. (a) A cell is selected by the operator. (b) Cell is recognized using Hough gradient transform. (c) Cell is visually servoed to the image center. White dots are cell trajectories. (d) Cell reaches the center of the image.

the speed of the cell is proportional to the fluid velocity, the cell accelerates when it enters the micropipette. On the other hand, the cell decelerates when it is dispensed out of the micropipette during cell deposition. Considering cell acceleration and the limited field of view of the microscope, well controlled cell aspiration is challenging since the cell can disappear far into the micropipette.

### B. Cell Recognition and Tracking

When the operator clicks on a selected cell, a region of interest (ROI) is created. Since the contour of a suspended cell is close to a circle, Hough gradient transform is applied to locate the maximum circle in the ROI. For every non-zero point found in Canny edge detection, the local gradient of these points are computed using a Sobel filter. The direction of the gradient at each edge point is used as additional information as the circle center  $(a, b)$  lies on the line passing through the edge point along the gradient direction. This method helps reduce the computation of accumulator from three-dimensions as in conventional Hough transform to two-dimensions. After the center  $(a, b)$  is found, the radius  $r$  is calculated by averaging the distances of every edge point to the circle center (Fig. 5(b)).

The identified cell is then automatically moved to the image center using image-based visual servoing. In order to obtain image feedback, a sum-of-squared-differences (SSD) tracking algorithm [15] is employed to track the cell. The template is obtained from the Hough gradient transform process. A search window of  $130 \times 130$  pixels is used. 30Hz tracking performance is readily achieved. Position differences between the cell center and the image center in the image space is used to visually servo the cell to the center of the field of view (Fig. 5(c)(d)).

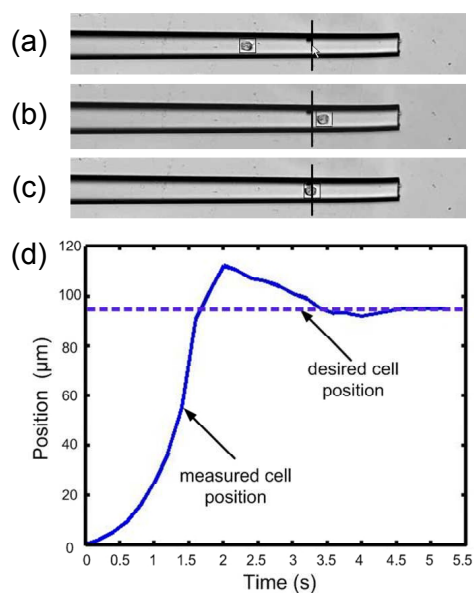


Fig. 6. (a)-(c) Closed-loop position control of a cell inside micropipette. (d) Step response.

### C. Cell Position Control inside Micropipette

When the system aspirates a cell, the position of the cell inside the micropipette must be controlled. The cell needs to be controlled to stop at a defined position that is very close to the micropipette opening, as shown in Fig. 6(c) for facilitating the subsequent dispensing operation at a target deposition location.

Fig. 7 shows the control diagram for cell position control. The system controls the motion of the linear stage to regulate the position of the plunger inside the syringe. Consequently, the air pressure and fluid velocity inside the micropipette vary, generating a force,  $F$  to move the cell. Let  $X_d$  be the desired position of the cell inside the micropipette, and  $X_c$  be the visually tracked cell center position, a PID controller is used for the positioning task.

As shown in Fig. 6(a), the cell ( $\sim 20 \mu\text{m}$ ) enters the micropipette tip ( $30 \mu\text{m}$  inner diameter) at a high speed, exceeding the reference/desired position. It took  $\sim 4.5\text{sec}$  for the cell to reach steady state (Fig. 6 (c)(d)). The controller would fail if the cell suddenly disappears from the field of view when a very high fluid velocity is induced. Thus, a threshold value  $v_T$  is set to the controller output. Cell speed  $v_c = 30\sqrt{(\Delta u)^2 + (\Delta v)^2}$ , where  $(\Delta u, \Delta v)$  is the displacement of the cell in two adjacent frames of image. When  $v_c > v_T$ , the PID controller's output is set to be zero. This thresholding restricts the fluid velocity at the micropipette tip; meanwhile, it also leads to long operation time for cell aspiration.

### D. Cell Aspiration Using a Holding Pipette

The use of micropipettes shown in Fig. 4(a) requires subtle control of picoliter volume of cell medium and ultra fine control of fluid pressure in order to obtain highly controlled aspiration of a cell inside the micropipette. This method

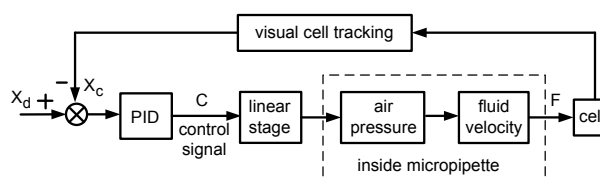


Fig. 7. Visual servo control to position a cell inside the micropipette.

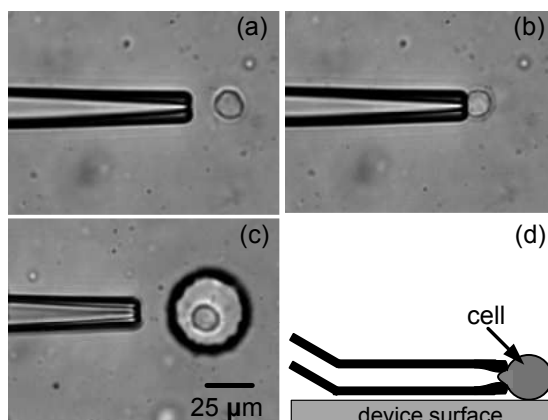


Fig. 8. (a)-(b) Pick up a cell using a holding micropipette with an opening of  $5 \mu\text{m}$ . (c) Place the cell into a target microwell. (d) Schematic illustration of the use of a holding micropipette to pick up a cell.

has the distinct advantage of non-invasiveness due to the direct manipulation of fluids. Based on 167 trials, the system obtained a success rate of 80.24%.

In order to improve the success rate, we produced micropipettes in the shape of a holding pipette, shown in Fig. 8(d). The micropipette has a small opening ( $5 \mu\text{m}$ ) to block a cell from completely entering the micropipette during aspiration. A low sucking pressure picks up a cell and aspirates a small portion of the cell slightly into the micropipette opening. The use of such a micropipette alleviates the intricacy of picoliter fluid control; however, sucking pressure must also be precisely controlled in order to hold the cell securely for transfer and also importantly, to be gentle enough without elongating too large a portion of the cell into the micropipette.

Required sucking pressure is  $\Delta P \approx P_0 \frac{L}{L_1}$ , where  $P_0$  is the atmospheric pressure,  $L_1$  is the length of the air bubble after aspiration, and  $L$  is the displacement of the plunger in the syringe controlled by the linear stage. In practice, since the micropipette is roughly half filled with mineral oil, it is difficult to accurately measure  $L_1$ . Thus, the appropriate range of aspiration pressures was determined experimentally. For example, for the aspiration of a porcine aortic valvular interstitial cell (PAVIC), a negative pressure of 180 Pa caused a cell elongation length of  $1 \mu\text{m}$  into the micropipette. Fig. 8(a)-(c) show the process of picking up a PAVIC cell from a source area and depositing it into a target microwell.

#### IV. RESULTS AND DISCUSSION

We have applied the system to pick-place single cells onto three types of microfabricated devices used in high-throughput cell biology research. In the first demonstration, single cells were deposited into microwell arrays made in polydimethylsiloxane (PDMS). Similar microdevices have been used to study stem cell differentiation and are ideal for probing cellular response to a large number of matrix protein factors [16]. Random cell settling using a diluted cell suspension has been shown at best to fill 80% of the wells with single cells (i.e., 20% of the wells contain either zero or multiple cells), and many cells ended up on the ridges between microwells. The method also is strongly dependent on experimental skills. Using the microrobotic manipulation system, we were able to readily fill microwell arrays with each microwell filled with one and only one cell. Fig. 1 shows an example array filled with PAVIC cells.

The second microdevice was designed to study cellular projections, consisting of an array of tightly constricting microfluidic channels and small cell culture chambers in the middle. The microdevice was used to simulate the physical constraints experienced by osteocytes (a type of bone cell) *in vivo*. The thin microchannels allow cells to extend themselves in a manner similar to that within the bone matrix. Single cells must be deposited into the multiple culture chambers for quantifying cellular response of many cells in parallel. The micromanipulation system was used to pick-place osteocytes precisely into desired locations. Fig. 9(a) shows one column within the microdevice, filled with single cells in each chamber. Deposited cells adhered to the protein matrix within the chambers. Fig. 9(b) shows cells projecting into the microchannels 3 hours after deposition (cytoskeleton stained green). Microfluidic flow can now be used to determine cellular response to mechanical/chemical stimulation.

The third microdevice was developed to study cellular response to mechanical substrate deformation [4]. The array, shown in Fig. 9(c) consists of a multi-layered PDMS structure, in which substrate deformations of different magnitudes are applied by raising micro loading posts. We attempted to incorporate single-cell handling structures into the device. However, these structures all interfered with the physical movement of the substrate. Furthermore, within a large area (a few hundred microns) on each element, there is only a small region (100  $\mu\text{m}$ ) that has uniform strain and is suitable to use, making the deposition of single cells in the correct positions challenging. Using the microrobotic system, we were able to deposit single progenitor cells at correct locations on the microdevice to enable experiments for determining the activation and translocation of a protein into the cell nucleus in response to substrate deformation.

In experiments, pick-place using both types of micropipettes was evaluated. Performance comparisons are summarized in Table I. Using the method of aspirating a cell into the micropipette, we achieved an average speed of 30 seconds for pick-place of one cell. Since the fluid velocity

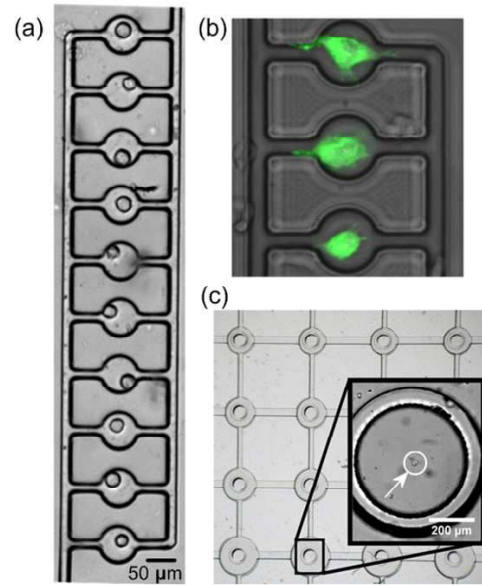


Fig. 9. (a) Osteocytes deposited into PDMS microarrays. (b) Cells extended into microchannels after they adhered on chamber bottom. (c) A  $4 \times 4$  microfabricated array of mechanically active substrates. Single cells were deposited on each unit in the array.

at the micropipette tip must be controlled to be low to avoid sucking the cell far into the micropipette, it takes averagely 20 seconds for a cell to move into the micropipette and for the controller to stabilize the cell's position to steady state.

After a cell is picked up, the  $X$ - $Y$  stage moves a microwell center to the center of the field of view. The distance between the location of cell sources and target microwells was approximately 1 mm. During the cell transfer process, the micropipette tip and cell both remained within cell culture medium. The speed of the stage was set to 1 mm/sec. During cell deposition, the cell decelerates when dispensed out of the micropipette tip. However, fine control of fluid velocity is still a must before the cell leaves the micropipette, in order for the cell to be accurately deposited at a target location. Experimentally, the speed was controlled to be lower than 50  $\mu\text{m}/\text{sec}$ . It took averagely 9 seconds to dispense a cell and for the cell to enter a microwell.

The success rate (pick up a cell and place it into a microwell) was 80.24%. The most often observed failures were caused by the micropipette wall that blocked a cell from entering the micropipette. For example, for a micropipette with a 30  $\mu\text{m}$  inner diameter, the wall thickness of the micropipette tip is  $\sim 5 \mu\text{m}$ . When the micropipette tip was positioned on the surface of a microdevice, a cell (8  $\mu\text{m}$ -18  $\mu\text{m}$ ) was sometimes blocked by the outer wall of the micropipette tip. In 19.76% of the experimental situations, a low fluid velocity was not able to overcome the blocking force, while a high fluid velocity caused the cell to disappear far into the micropipette, both resulting in failures.

When a holding pipette was used for pick-place of cells, the average speed was 15 seconds (Table I). It typically only took 3 seconds to pick up a cell. However, it took

TABLE I  
PERFORMANCE COMPARISONS OF CELL HOLDING AND CELL  
ASPIRATION TECHNIQUES

	Cell Aspiration	Cell Holding
Pickup Time	20 sec	3 sec
Transfer Time	1 sec	5 sec
Place Time	9 sec	7 sec
Success Rate	80.24% (n = 167)	95.13% (n = 185)

~5 seconds to transfer the cell across the 1 mm distance because the speed of the X-Y stage had to be set low, such as 200  $\mu\text{m}/\text{sec}$ . Otherwise, a high motion speed of the stage generated turbulence in the cell medium, causing the micropipette to lose the gently held cell. It averaged 7 seconds to place a cell to a target location. Since the cell is in direct contact with the micropipette wall, adhesion must be overcome before the cell is successfully deposited. Sigmacote (Sigma-Aldrich, Canada) was used to coat the micropipette prior to use to reduce adhesion. Micropipette tips were dipped into a vial of Sigmacote for 1-2 seconds. Air was then pushed through the micropipette to clear the tip of excess solution. Pipettes were allowed to dry for several hours in a fumehood before use. This treatment was found to substantially reduce cell adherence to the glass micropipette, facilitating controlled deposition. The success rate using a holding micropipette for cell deposition was 95.13%.

Overall, this study demonstrates that holding a cell against the micropipette wall (i.e., using a holding micropipette) produced both a higher operation speed (15 seconds per cell vs. 30 seconds per cell) and a higher success rate (80.24% vs. 95.13%) than aspirating a cell inside the micropipette (i.e., the use of a micropipette with large openings). Therefore, for pick-place of most types of cells, the cell holding approach is a more efficient technique than the cell aspiration method. However, it must be noted that for handling highly delicate or sensitive cell types, such as embryonic stem cells and induced pluripotent stem cells, which are responsive to both biochemical and mechanical stimulations, aspirating cells into the micropipette may be a better approach that directly manipulates picoliter fluids, which should produce a lower level of mechanical stimulation.

## V. CONCLUSION

This paper presented a micromanipulation system for automated pick-place of single cells. A user, without skill requirements, operates the system by selecting an appropriate cell for pick-place via computer mouse clicking. The system picks up a cell and deposits it at a target location at a speed of 15-30 seconds. The system integrates computer vision and motion control algorithms, having the advantages of non-invasiveness, high specificity, and high precision. It is suitable to pick-place both non-labeled and labeled cells

and applicable to any standard cell culture substrates and microdevices with an open top.

Microrobotic pick-place of single cells is a serial process and may be most suitable to use in combination with other parallel, yet less precise/specific techniques. For example, random settling [6] and the bio flip chip technique [17] are parallel processes for depositing many cells rapidly with an approximate success rate of 70%-80%. After the application of these parallel techniques, the microrobotic system can be used to fill single cells into a limited number of empty locations, clean up those cells that end up on ridges between two target locations, or remove cells from a microwell that contains more than one cell. Such a combined use of parallel techniques and microrobotic manipulation will promise high efficiency and success rates for large-scale operation.

## VI. ACKNOWLEDGMENTS

This work was supported by the Natural Sciences and Engineering Research Council of Canada and the Ontario Ministry of Research and Innovation.

## REFERENCES

- [1] D. G. Anderson, D. Putnam, E. B. Lavik, T. A. Mahmood, and R. Langer, "Biomaterial microarrays: rapid, microscale screening of polymer-cell interaction," *Biomaterials*, vol. 26, pp. 4892-4897, 2005.
- [2] R. Gomez-Sjoberg, A. A. Leyrat, D. M. Pirone, C. S. Chen, and S. R. Quake, "Versatile, fully automated, microfluidic cell culture system," *Anal. Chem.*, vol. 79, no. 22, pp. 8557-8563, 2007.
- [3] C. J. Flaim, D. Teng, S. Chien, and S. N. Bhatia, "Combinatorial signaling microenvironments for studying stem cell fate," *Stem Cells Dev.*, vol. 17, no. 1, pp.29-39, 2008.
- [4] C. Moraes, C. A. Simmons, and Y. Sun, "A high-throughput array for mechanical stimulation of adherent biological cells," *IEEE Int. Conf. Solid-State Sensors, Actuators and Microsystems*, Denver, CO, 2009.
- [5] S. Raghavan, and C. S. Chen, "Micropatterned environments in cell biology," *Adv. Mater.* vol. 16, pp. 1303-1313, 2004.
- [6] J. R. Rettig and A. Folch, "Large-scale single-cell trapping & imaging using microwell arrays," *Anal. Chem.*, vol. 77, pp. 5628-34, 2005.
- [7] M. Hosokawa, A. Arakaki, M. Takahashi, T. Mori, H. Takeyama, and T. Matsunaga, "High-density microcavity array for cell detection: single-cell analysis of hematopoietic stem cells in peripheral blood mononuclear cells," *Anal. Chem.*, vol. 81, no. 13, pp. 5308-5313, 2009.
- [8] T. P. Hunt and R. M. Westervelt, "Dielectrophoresis tweezers for single cell manipulation," *Biomed. Microdevices*, vol. 8, pp. 227-230, 2006.
- [9] D. DiCarlo, N. Aghdam, and LP. Lee, "Single-cell enzyme concentrations, kinetics, and inhibition analysis using high-density hydrodynamic cell isolation arrays," *Anal. Chem.*, vol. 78, pp.4925-30, 2006.
- [10] A. Ashkin, J. M. Dziedzic, and T. Yamane, "Optical trapping and manipulation of single cells using infrared laser beams," *Nature*, vol. 330, pp. 769-771, 1987.
- [11] L. Gherardini, C. M. Cousins, J. J. Hawkes, J. Spengler, S. Radel, H. Lawler, B. Devic-Kuhar, and M. Groschl, "A new immobilisation method to arrange particles in a gel matrix by ultrasound standing waves," *Ultrasound Med. Biol.*, vol. 31, pp. 261-272, 2005.
- [12] C. Wilhelm, F. Gazeau, and J. C. Bacri, "Magnetic micromanipulation in the living cell," *Europhys. News*, vol. 33, pp. 89-92, 2005.
- [13] Y. H. Anis, M. R. Holl, and D. R. Meldrum, "Automated vision-based selection and placement of single cells in microwell array formats," in *Proc. Int. Conf. Autom. Sci. Eng.*, pp. 315-320, 2008.
- [14] W. H. Wang, X. Y. Liu, and Y. Sun, "Contact detection in microrobotic manipulation," *Int. J. Robot. Res.*, vol. 26, pp. 821-828, 2007.
- [15] K. Nickels and S. Hutchinson, "Estimating uncertainty in ssd-based feature tracking," *Image Vision Comput.*, vol. 20, pp. 47-58, 2002.
- [16] V. I. Chin, P. Taupin, S. Sanga, J. Scheel, F. H. Gage, and S. N. Bhatia, "Microfabricated platform for studying stem cell fates," *Biotechnol. Bioeng.* vol. 88, no. 3, pp. 399-415, 2004.
- [17] A. Rosenthal, A. Macdonald, and J. Voldman, "Cell patterning chip for controlling the stem cell microenvironment," *Biomaterials*, vol. 28, pp. 3208-3216, 2007.